BEAM COUPLING IMPEDANCE IN THE ILC DAMPING RINGS*

M. Korostelev†, A. Wolski, University of Liverpool and the Cockcroft Institute, UK
O.B. Malyshev, STFC ASTeC and the Cockcroft Institute, UK
A.F. Grant, J. Lucas, STFC Technology, Daresbury Laboratory, UK

Abstract

The damping rings of the International Linear Collider (ILC) have stringent specifications for beam quality and stability. To avoid instabilities, the various components in the vacuum chamber will need to be carefully designed to minimize the longitudinal and transverse wake fields. We present the results of impedance calculations for BPM insertions that are expected to make a significant contribution to the overall machine impedance.

DAMPING RING BPMS

In the present configuration, the ILC damping rings [1] have circumference 6476 m and beam energy 5 GeV. A lattice has recently been developed that has momentum compaction factor around 2×10^{-4}; this is significantly lower than the previous specification of 4×10^{-4}, and allows the machine to operate with reduced rf voltage and shorter bunch length. The reduced rf voltage helps reduce the costs of the damping rings themselves while the shorter bunch helps to reduce the costs of the bunch compressors downstream of the damping rings. However, the lower momentum compaction factor assumes that a very low machine impedance can be achieved, so as to operate below the threshold of single-bunch instabilities.

There are also demanding requirements on the orbit and coupling correction system: in order to achieve a vertical emittance of 2 pm, a large number of high performance beam position monitors (BPMs) will be needed [2]. The total number of BPMs may be as large as 690, and they are expected to make a significant contribution to the machine impedance. Understanding the impedance of the BPM insertions (that include bellows, flanges, and sections of vacuum chamber tapering to antechambers) is therefore important for developing a design capable of meeting the overall performance specifications. In this paper, we report the results of calculations of the impedance using the code HFSS applied to technical designs of the BPM insertions.

Fig. 1 shows a cut-away section of one BPM insertion, including bellows, flanges and antechamber taper. The bellows provide mechanical isolation of the housing for the BPM buttons from the main vacuum chamber, and are shielded by stainless steel screens to reduce impedance. The cylindrical vacuum chamber in the arcs has a rectangular antechamber to reduce the number of photons in the main chamber: this is intended to help suppress electron cloud effects in the positron damping ring, and may also help improve the vacuum and reduce ion effects in the electron damping ring. However, there is no antechamber in the BPM insertion, to minimise the risk of propagating modes; the antechamber is tapered smoothly (over 750 mm) either side of each BPM. To shield the BPMs from synchrotron radiation, the button housing has a slightly larger diameter than that in the section of chamber on either side. The full horizontal and vertical apertures are 80 and 62 mm, respectively.

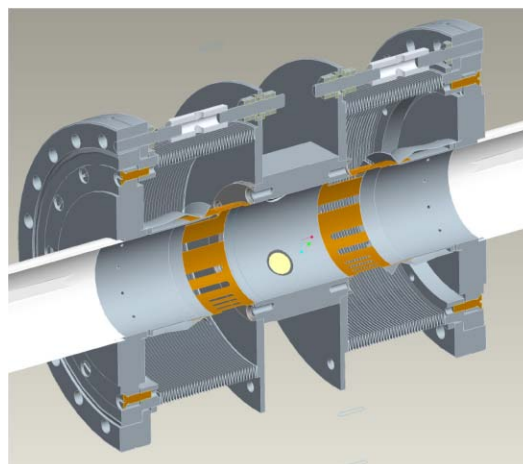

Figure 1: BPM insertion.

The BPM pick-ups are shown in more detail in Fig. 2; they consist of four buttons arranged at 45° to the horizontal and vertical axes. The buttons are scaled from a model developed for PEP-II [3]. Each button has diameter 8 mm, and there is a gap of 1 mm between the button and its housing. An alumina glass ring is used for vacuum insulation. All pick-ups are terminated by SMA-type (sub-miniature) connector, matched to the impedance of a 50 Ω coaxial line.

IMPEDANCE CALCULATIONS

Coaxial Wire Method

The model shown in Fig. 1, including antechamber tapers on either side, is used for the impedance calculations. Its total length is 228.8 cm. The impedance was calculated using the 3D electromagnetic modelling code HFSS [4]. Unlike codes such as MAFIA and GdfidL, HFSS does not provide the beam wake potential directly. However, by sweeping the signal frequency across a wide spectrum, we

* Work supported by the Science and Technology Facilities Council.
† m.korostelev@cockcroft.ac.uk

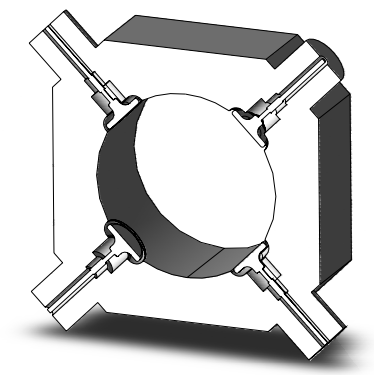

Figure 2: Cross-section of vacuum chamber showing BPM button-style pick-ups.

can calculate the impedance as a function of frequency; the wake potential is obtained as the Fourier transform of the impedance.

Our calculations are based on the coaxial wire method. The basic idea is as follows: the field excitation from a short relativistic beam travelling through some "device under test" (DUT) is represented by a transverse electromagnetic (TEM) wave around thin wire stretched inside the DUT along the reference beam trajectory. Thus, any vacuum chamber component can be represented as a coaxial transmission line. The impedance of a transmission line can be characterized by its transmission parameters (S-parameters), which depend upon the transmission line structure, the characteristic impedances of the wave ports, and the frequency.

Longitudinal Impedance and Loss Factor

There are a number of approximate formulae that can be used to express the longitudinal coupling impedance of a DUT as a function of the S-parameters. In our calculation, we use the "improved log formula", which is widely used for long devices and/or high frequencies:

$$Z_{\parallel} = -2Z_c \ln \frac{S_{21}^{\mathrm{DUT}}}{S_{21}^{\mathrm{REF}}} \left(1 - \frac{1}{2\gamma d} \ln \frac{S_{21}^{\mathrm{DUT}}}{S_{21}^{\mathrm{REF}}}\right), \quad (1)$$

where S_{21}^{DUT} is the transmission parameter of the DUT, and S_{21}^{REF} is the transmission parameter of an ideal reference transmission line of the same length d as the DUT. Z_c and γ are the characteristic impedance and the propagation constant of transmission line, respectively. Usually, if $\omega d/c > 1$, Eq. (1) is in good agreement with real rf measurements performed by the wire method.

In our case, the reference transmission line is a straight section of the "wired" cylindrical beam pipe, with length 2.288 m and diameter 62 mm. The transmission parameter S_{21} refers to the amplitude of the signal exiting the transmission line, compared to the amplitude of the signal entering the transmission line.

Fig. 3 shows the amplitude of the S_{21} parameter of the BPM insertion up to 40 GHz, computed using HFSS. Above a certain cut-off frequency, transverse electric and/or transverse magnetic modes can propagate in the coaxial transmission line, just as they do in a cylindrical waveguide; this may result in interference between multiple modes with different phase velocities.

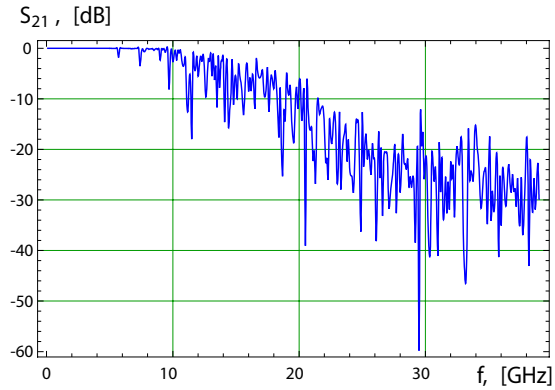

Figure 3: Transmission parameter S_{21} of the BPM insertion.

Direct comparison of the frequency spectra of the reference transmission line and the DUT is not usually sufficient to distinguish clearly all the actual resonances of the DUT, since the resonant frequency for higher-order modes of identical types in the reference transmission line and the DUT can be somewhat different.

Figs. 4 and 5 show respectively, the real and imaginary parts of the longitudinal impedance of the BPM insertion, obtained from Eq. (1) applied to the transmission parameter shown in Fig. 3.

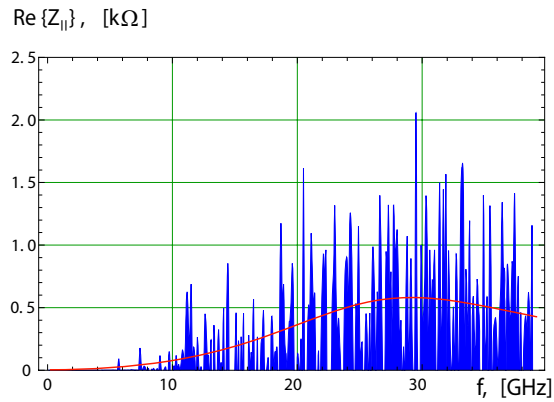

Figure 4: Real part of the longitudinal impedance of the BPM insertion. The red line indicates a broad-band approximation.

The real part of the longitudinal impedance represents the energy loss for a bunch with a Gaussian distribution. The total rate of energy loss for the beam is given by:

$$P = e^2 n_e^2 n_b f_{rev} k_{\parallel}.$$

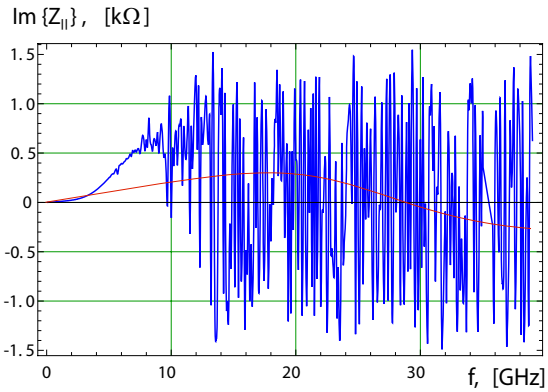

Figure 5: Imaginary part of the longitudinal impedance of the BPM insertion. The red line corresponds to a broad-band approximation.

Here, n_e and n_b are the bunch population and the number of bunches, respectively, and the loss factor $k_\parallel$ is given by:

$$k_\parallel = \frac{1}{\pi}\int_0^\infty \mathrm{Re}\, Z_\parallel(\omega)\, e^{-\omega^2\sigma_\tau^2}\, d\omega.$$

Assuming that the nominal bunch length $\sigma_s = 6$ mm ($\sigma_\tau = 20$ ps), the loss factor per BPM insertion is 0.76 V/pC. Thus, the average dissipated power per BPM insertion in the ILC damping rings (with $n_e = 2\times10^{10}$, $n_b = 2610$) is 940 W.

Transverse Impedance and Kick Factor

From the Panowsky-Wenzel theorem, the transverse impedance can be expressed as:

$$Z_\perp \simeq \frac{c}{\omega}\cdot\frac{Z_\parallel(x_1) - Z_\parallel(x_0)}{(x_1-x_0)^2}.$$

Thus to find the transverse impedance, we computed the longitudinal impedance as a function of the transverse displacement of the wire.

Knowledge of the imaginary part of the transverse impedance allows us to calculate the kick factor $k_\perp$ for a Gaussian beam, defined by

$$k_\perp = -\frac{1}{\pi}\int_0^\infty \mathrm{Im}\, Z_\perp(\omega)\, e^{-\omega^2\sigma_\tau^2}\, d\omega. \qquad (2)$$

The transverse kick deflects a bunch by:

$$\theta = r_e n_e x_0 k_\perp/\gamma,$$

where x_0 is the beam offset with respect to the longitudinal axis, and γ is the relativistic factor. Using Eq. (2), we obtain $k_{\perp x} = 3.1$ V/pC/m for the horizontal kick factor, and $k_{\perp y} = 8.4$ V/pC/m for the vertical kick factor.

Broad-Band Impedance

The longitudinal impedance of a vacuum chamber component can be approximated, in a broad-band model, by a single mode cavity (resonant LCR-circuit):

$$Z_{bb}(\omega) = \frac{R_s}{1 + iQ(\frac{\omega}{\omega_r} - \frac{\omega_r}{\omega})}. \qquad (3)$$

The quality factor is usually taken as $Q = 1$. The resonant frequency ω_r and shunt impedance R_s can be tuned to reproduce the loss factor of the component of interest, in our case a BPM insertion. We find that appropriate values of these parameters for the model used here are $\omega_r \approx 2\pi\cdot 29$ GHz and $R_s \approx 600\,\Omega$. The real and imaginary parts of the broad-band impedance are shown as red lines in Figs. 4 and Fig. 5, respectively.

An indication of beam stability in the presence of a broad-band impedance can be found from the Keil-Schnell-Boussard criterion:

$$\left|\frac{Z}{n}\right|_{bb} < Z_0\sqrt{\frac{\pi}{2}}\frac{\gamma\alpha_p\sigma_\delta^2\sigma_z}{r_e n_e}. \qquad (4)$$

An effective broad-band impedance can be expressed as a low-frequency limit:

$$\left|\frac{Z}{n}\right|_{bb} = \lim_{\omega\to0}\left|\frac{Z(\omega)}{n}\right| = \omega_{rev}L,$$

where $n = \omega/\omega_{rev}$, and using Eq. (3) $L = R_s/\omega_r Q$. With the above values for R_s and ω_r, we find $L \approx 3.5$ nH; this leads to an effective broad-band impedance of around 1 mΩ per BPM insertion. For 690 BPMs, the total broad-band impedance would be around 690 mΩ; whereas the Keil-Schnell-Boussard criterion Eq. (4) with $\sigma_\delta = 1.3\times10^{-3}$ gives an instability threshold of around 170 mΩ. While it appears that the damping rings would operate above the instability threshold, it should be remembered that the Keil-Schnell-Boussard criterion gives only a crude estimate, and more detailed modelling of the dynamics will be needed to determine the instability threshold with greater reliability.

ACKNOWLEDGEMENT

We thank Cho Ng for providing us with the original model of the BPM buttons.

REFERENCES

[1] https://wiki.lepp.cornell.edu/ilc/pub/Public/DampingRings/WebHome/

[2] K. Panagiotidis and A. Wolski, "Coupling correction for the ILC damping rings," these proceedings (2008).

[3] N. Kurita et al, "Design of the button beam position monitor for PEP-II," SLAC-PUB-95-6991, published in Proceedings of PAC95, Dallas, Texas, USA (1995).

[4] Ansoft Corporation, http://www.ansoft.com